Quaternary Science Reviews 312 (2023) 108147

Contents lists available at ScienceDirect

Quaternary Science Reviews

journal homepage: www.elsevier.com/locate/quascirev

^{10}Be exposure ages and paleoenvironmental significance of rock glaciers in the Western Tatra Mts., Western Carpathians

Tereza Dlabáčková [a, b, *], Zbyněk Engel [a], Tomáš Uxa [c], Régis Braucher [d], Aster Team [d, 1]

[a] Faculty of Science, Charles University, Prague, Czech Republic
[b] Czech Geological Survey, Prague, Czech Republic
[c] Institute of Geophysics, Czech Academy of Sciences, Prague, Czech Republic
[d] CEREGE CNRS Aix Marseille Univ., IRD, INRAE, Collège de France, Aix-en-Provence, France

ARTICLE INFO

Article history:
Received 25 March 2023
Received in revised form
17 May 2023
Accepted 19 May 2023

Handling editor: Claudio Latorre

Keywords:
Quaternary
Lateglacial
Cosmogenic isotopes
Paleoclimatology
Permafrost
Europe

ABSTRACT

Relict rock glaciers are well-preserved features of high-elevated valleys in the Western Tatra Mts., Western Carpathians, but their chronology remained poorly constrained with numerical dating methods. We present the first robust set of ^{10}Be exposure ages for eight rock glaciers with front elevation of 1376–1819 m asl. The results suggest that the rock glaciers stabilized throughout the Weichselian Lateglacial from ~16.5 ka to 11 ka. This timing is consistent with the period of rock glacier stabilization in European mountain regions, but it extends the age span previously determined for rock glaciers in the Tatra Mts. There are differences between north- and south-facing valleys in the elevation and time of the stabilization of the rock glaciers, which were probably caused by contrasts in potential incoming solar radiation that affected the retreat of former glaciers and the subsequent formation of the rock glaciers. The initiation altitude of ~1610 and ~1830 m asl determined for the oldest and youngest dated rock glaciers is generally consistent with previous estimates of the glacier equilibrium line altitude during the Greenland Stadials 2.1 and 1, respectively. However, the lower limit of the rock glaciers is well above regional paleopermafrost features from the same periods, which suggests that rock glaciers may underestimate past permafrost extents and temperature declines disputing their regional validity for paleoenvironmental reconstructions.

1. Introduction

Rock glaciers are thick lobate- or tongue-shaped masses of angular debris and ice that move slowly down high mountain slopes due to the deformation of the internal ice, which also causes the formation of a typical surface relief of rock glaciers consisting of transverse and longitudinal ridges and furrows (Barsch, 1996; French, 2017; Ballantyne, 2018). The internal ice may be of permafrost or glacial origin (Whalley and Martin, 1992; Jones et al., 2019) as rock glaciers represent landforms formed by glacial and/or periglacial processes (e.g. Janke et al., 2013). The debris is derived from adjacent talus slopes for so-called talus rock glaciers or moraine deposits covering valley floors for so-called debris rock glaciers (Barsch, 1996; Ballantyne, 2018). Active rock glaciers are supposed to form and move in regions with low precipitation and mean annual air temperature (MAAT) <−2 °C (Barsch, 1996; Humlum, 1998). At higher temperatures, topographic constraints or limited debris supply, their activity ceases and they turn into inactive rock glaciers, and if the ice core melts completely they become relict rock glaciers (Barsch, 1996; Kääb, 2013). Consequently, the individual types of rock glaciers tend to be located at elevation zones, which correspond to specific climatic conditions. Elevation of rock glacier fronts has thus been widely used as a proxy indicator for present and past lower limit of discontinuous permafrost or for past climatic conditions in which the rock glaciers formed and were active (Frauenfelder et al., 2001). Relict rock glaciers are valuable in that they can provide a proxy record of past environmental conditions where other natural archives, such as lake sediments, may be incomplete. Determining the age of relict rock glaciers is thus important for understanding the postglacial evolution of mountain relief, especially in the Tatra Mts., where this

* Corresponding author. Faculty of Science, Charles University, Albertov 6, Prague 2, 128 00, Czech Republic.
E-mail address: tereza.dlabackova@natur.cuni.cz (T. Dlabáčková).
[1] Aster Team: Georges Aumître, Fawzi Zaidi, Karim Keddadouche.

https://doi.org/10.1016/j.quascirev.2023.108147

period of landscape development has not yet been sufficiently explored.

The age of rock glaciers has formerly been determined using several methods of relative dating such as measuring the surface weathering of rock boulders with the Schmidt hammer (Frauenfelder et al., 2005; Kellerer-Pirklbauer, 2008a, 2008b; Kłapyta, 2011, 2013; Zasadni and Kłapyta, 2016; Zasadni et al., 2020), weathering rind thickness (Laustela et al., 2003), lichenometry (Haeberli et al., 1979; Hamilton and Whalley, 1995; Nicholas and Butler, 1996; Refsnider and Brugger, 2007) or alternatively by photogrammetric and geodetic measurements of the rock glacier flow (Kääb et al., 1998; Vespremeanu-Stroe et al., 2012). However, recent decades have seen an expansion in numerical dating methods using radionuclides ^{14}C preserved in organic remnants buried by rock glaciers (e.g. Scapozza et al., 2010; Krainer et al., 2015) and cosmogenic radionuclides ^{36}Cl (e.g. Palacios et al., 2015; Moran et al., 2016; Fernández-Fernández et al., 2020) and ^{10}Be (e.g. Ivy-Ochs et al., 2009; Steinemann et al., 2020; Zasadni et al., 2020) in surface boulders on rock glaciers. A combination of relative and numerical dating methods has also widely been used for so-called Schmidt hammer exposure-age dating (Rode and Kellerer-Pirklbauer, 2012; Matthews et al., 2013; Matthews and Winkler, 2022).

Cosmogenic exposure dating of rock glaciers in Europe has so far been carried out in the Iberian Peninsula (Palacios et al., 2015, 2016; Rodríguez-Rodríguez et al., 2016, 2017; Andrés et al., 2018; García-Ruiz et al., 2020; Santos-González et al., 2022), the Alps (Ivy-Ochs et al., 2006, 2009; Hippolyte et al., 2009; Böhlert et al., 2011; Moran et al., 2016; Steinemann et al., 2020; Charton et al., 2021), Tröllaskagi Peninsula, Iceland (Fernández-Fernández et al., 2020; Palacios et al., 2021), Øyberget, Norway (Linge et al., 2020), Cairngorm Mts., Great Britain (Ballantyne et al., 2009), or the Romanian Carpathians (Vasile et al., 2022). Most authors attributed the exposure age of rock glaciers to a period of their stabilization, which started no earlier than in the Greenland Stadial 2.1a (GS-2.1a) (Rodríguez-Rodríguez et al., 2016; Steinemann et al., 2020; Ballantyne et al., 2009) and continued until the mid-Holocene at the latest (Palacios et al., 2016, 2021).

However, dating of rock glaciers in some other European regions, such as the Tatra Mts., Western Carpathians, has been limited. The age of rock glaciers in the Tatra Mts. was initially deduced based on paleoclimatic considerations and relative dating methods. Kotarba (1992) claimed based on paleoclimatic reconstructions that rock glaciers in the Tatra Mts. formed during the Greenland Stadial 1 (GS-1) (~Younger Dryas). Several authors extended the age span of rock glaciers in the Tatra Mts. using the Schmidt hammer test to the entire Lateglacial (Kłapyta, 2011, 2013; Zasadni and Kłapyta, 2016; Zasadni et al., 2020), but these estimates have not yet been fully confirmed by numerical dating. For the Western Tatra Mts., there is only one study providing exposure ages of ~13 and ~12 ka for the stabilization of rock glaciers (Engel et al., 2017). In the High Tatra Mts., Zasadni et al. (2020) dated the final phase of stabilization of the highest-elevated rock glaciers in cirques to the end of the GS-1 to early Holocene. However, numerical ages for the stabilization of lower-elevated and probably older rock glaciers are still lacking.

The main objective of this study is to determine the chronology of the stabilization of rock glaciers in the Western Tatra Mts. using ^{10}Be exposure dating. We hypothesize that the lowest-lying rock glaciers at ~1400 m asl could represent the period of early deglaciation after the local last glacial maximum (LGM) and those in high-lying cirques at ~1800 m asl could be from the beginning of the Holocene. We also compare the rock glacier chronology with similar investigations on rock glaciers as well as with other local and regional paleoenvironmental records.

2. Study area

The Western Tatra Mts. (the highest peak Bystrá at 2248 m asl) together with the High Tatra Mts. (2654 m asl) and the Belianske Tatra Mts. (2152 m asl) represent the northernmost part of the Carpathian arch, situated on the Slovak-Polish border (Fig. 1). The main ridge of the Western Tatra Mts. stretches in a roughly west-east direction for 42 km (the entire mountain chain is ~70 km long), while the maximum width of the mountain range is 16 km.

The Western Tatra Mts. are mainly composed of crystalline rocks of the Paleozoic age (State Geological Institute of Dionýz Štúr, 2013). Most of the mountain range consists of igneous rocks (granitoids), but the southern and northern parts are built of metamorphic rocks (mica schists, gneisses). In the outer areas of the mountain range, especially in the north, the crystalline rocks are overlain by Mesozoic sedimentary rocks (limestones, sandstones) (State Geological Institute of Dionýz Štúr, 2013; Králiková et al., 2014). The Western Tatra Mts. are bounded in the south by the sub-Tatra fault, along which the southern crests were uplifted to slightly higher elevations than the northern ones. The largest uplift accelerated from the end of the Late Miocene to the Pleistocene (Baumgart-Kotarba and Králˇ, 2002; Králiková et al., 2014; Jacko et al., 2021; Vitovič et al., 2021) and has continued into the postglacial period as documented by post-LGM fault scarps (Pánek et al., 2020). The Western Tatra Mts. are ~300 m lower compared to the High Tatra Mts., which is due to the asymmetrical rise of the

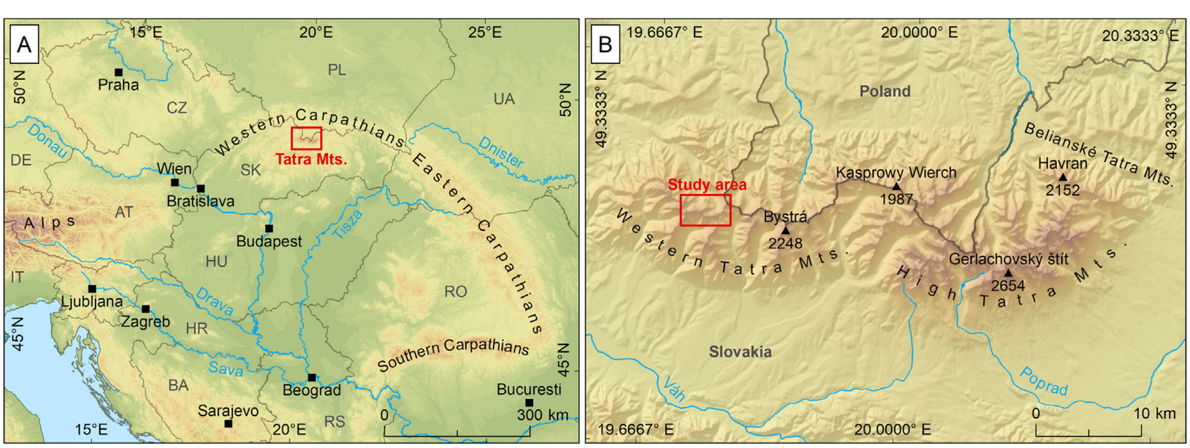

Fig. 1. Location of (A) the Tatra Mts. within the Carpathians and (B) the study area in the Tatra Mts.

individual blocks of the mountain range in the west-east direction (Baumgart-Kotarba and Král̆, 2002; Jurewicz, 2007; Králiková et al., 2014).

The Tatra Mts. were glaciated several times during the cold phases of the Pleistocene as indicate sequences of glacial and glaciofluvial sediments in front of the mountains (Lindner et al., 2003). The last glacial episode culminated during the local LGM, which terminated before ~18 ka in the Western Tatra Mts. (Engel et al., 2017). During the subsequent Lateglacial period, at least two stillstands or re-advances occurred in north-facing valleys (Makos et al., 2016; Engel et al., 2017). Nowadays, glaciers are no longer present, as the climatic snowline is estimated at 2500–2600 m asl on the northern slopes and at 2700–2800 m asl on the southern ones (Zasadni and Kłapyta, 2009); only firn-ice patches or perennial snowfields persist (Gądek, 2014). The lower limit of discontinuous permafrost is estimated at 1930 ± 150 m asl, depending on the local relief (Dobiński, 2005).

The Western Tatra Mts. represent a significant barrier to the air masses flowing from the northwest to the southeast, causing climatic differences between the northern and southern slopes (Niedźwiedź, 1992). The MAAT in the northern and southern foothills was approximately 6 °C and 8 °C in 1991–2010, respectively (Niedźwiedź et al., 2015; Żmudzka et al., 2015). The ridge part experienced the MAAT of approximately −2 °C to 0 °C in the same period (Żmudzka et al., 2015), and the mean annual precipitation was >1800 mm in 1981–2010 (Ustrnul et al., 2015). Rainfall constitutes major part of the annual precipitation, but snowfall events can occur at any time of the year. The number of days with solid precipitation ranges from 80 at the foothills to 165 in the summit zone (Niedźwiedź, 1992). Snow cover lasts 120–130 days in the valleys and more than 220 days on the highest peaks (Niedźwiedź et al., 2015). The number of days with snow cover at the Kasprowy Wierch (1991 m asl) varied from 199 to 268 and the maximum snow depth ranged from 140 cm to 325 cm during the 1998–2010 period (Gądek, 2014). The snow cover duration and depth in the Tatra Mts. has been decreasing since the mid-twentieth century due to climate warming and reduced snowfall (Gądek, 2011).

The study area is situated in the central part of the Western Tatra Mts. on the northern and southern slope of the main ridge (Figs. 1 and 2). The ridge area is built mainly of biotite granodiorite-tonalite to muscovite-biotite granodiorite (High Tatra Type), but porphyritic granitoid and leucogranite prevail around the Volovec and Rákoň peaks (Nemčok et al., 1994). The bedrock is overlain by extensive talus cones on the lower parts of the slopes and foothills, which are dissected by numerous debris flows (Kłapyta, 2015; Dlabáčková and Engel, 2022). The valley floors are filled with rock glaciers or glacigenic sediments (Kłapyta, 2009, 2011, 2013, 2015; Engel et al., 2017; Uxa and Mida, 2017; Zasadni et al., 2022). The Smutná and Spálená valleys on the north side of the main ridge are among the best developed glacial landscapes within the Western Tatra Mts. (Engel et al., 2017). However, deeply incised cirques also form the upper part of the Žiarska and Jamnícka valleys (Fig. 2).

3. Methods

3.1. Rock glacier selection

Eight rock glaciers spanning from low-lying valley bottoms to high-lying cirques oriented north and south of the main ridge of the Western Tatra Mts. were selected for exposure dating. The diagnostic features used to identify the rock glaciers were their distinctive morphology with steep fronts, transverse and longitudinal ridges and furrows, which indicate former downslope movement of the debris material (Barsch, 1996; RGIK, 2022).

The identification of the rock glaciers was based on LiDAR digital elevation model (DEM) with a horizontal resolution of 1 m (ÚGKK SR, 2018) as well as orthophotos with a resolution of 0.2 m (GKÚ Bratislava, 2021). All the delineated rock glaciers were checked and modified by field mapping in 2019–2021, the existing inventory of rock glaciers of the Tatra Mts. (Uxa and Mida, 2017) and previous studies from the study area (Nemčok and Mahr, 1974; Kłapyta, 2009, 2011, 2013, 2015; Engel et al., 2017). For each delineated rock glacier, elevation, flowline length and orientation, width, area, surface slope, front height and slope, and potential incoming solar radiation were determined from the DEM in accordance with conventional procedures (e.g. Barsch, 1996; Kellerer-Pirklbauer et al., 2012; Colucci et al., 2016). The rock glaciers were classified based on length-to-width ratio as lobate- (<1) and tongue-shaped (>1; Barsch, 1996). Their activity was assessed based on the presence of vegetation and soil cover (Barsch, 1996; Kääb, 2013) and the mean slope of the front (≤35° for relict rock glaciers; Haeberli, 1985; Barsch, 1996; Ballantyne, 2018).

The MAAT at the front of the rock glaciers was derived using a multiple linear regression based on the data collected during the period 1951–1970 at twenty weather stations (703–2635 m asl) in the Tatra Mts. (Niedźwiedź, 1992) as follows:

$$\mathrm{MAAT} = \beta_0 + \beta_1 x + \beta_2 y + \beta_3 z \tag{1}$$

where x (°) is the longitude, y (°) is the latitude, z (m) is the elevation, β_0 (47.3913 °C) is the regression intercept, and β_1 (0.8751 °C·°lon^{-1}), β_2 (−1.1335 °C·°lat^{-1}) and β_3 (−0.0047 °C·m^{-1}) is the longitudinal, latitudinal, and elevational air temperature gradient, respectively. The regression relationship explains 95% of the variability in MAAT and yields a mean absolute error of 0.44 °C. Additionally, it fits MAAT from the period 1981–2010 at the Kasprowy Wierch (1991 m asl), which is the closest high-elevated weather station with recent air temperature records available.

Since rock glaciers actively form at MAAT <−2 °C (Barsch, 1996; Kääb, 2013), the difference between this temperature threshold and the present MAAT at the front of the rock glaciers was used to estimate the minimum temperature decline when the rock glaciers stabilized (Frauenfelder et al., 2001). The corresponding minimum decrease of the lower limit of discontinuous permafrost was estimated from the elevation difference between the front of the rock glaciers and the present level of the −2 °C mean annual isotherm (~present lower limit of discontinuous permafrost) derived from Eq. (1) rearranged as follows:

$$z_{\mathrm{MAAT}=-2\,^{\circ}\mathrm{C}} = \frac{\mathrm{MAAT} - \beta_0 - \beta_1 x - \beta_2 y}{\beta_3} \tag{2}$$

which yields the present lower limit of discontinuous permafrost at ~2320 m asl.

3.2. Boulder sampling and sample treatment

A total of 34 rock samples were collected for exposure dating of the eight rock glaciers. Three to six boulders were sampled at each rock glacier to minimize the impact of choosing a boulder with a complex exposure history (Denn et al., 2018). We selected only flat-topped boulders higher than 1 m with no signs of erosion that were located on low-angled transverse ridges near the front of the rock glaciers. Samples were collected from the top surface of the boulders with a hammer and chisel. Sample locations and elevations were recorded using a handheld GPS receiver with ~2 m horizontal accuracy.

The samples were crushed, sieved and cleaned with a mixture of HCl and H_2SiF_6. The extraction method for ^{10}Be ($T_{1/2}$ = 1.387 ± 0.017 Ma; Chmeleff et al., 2010; Korschinek et al., 2010)

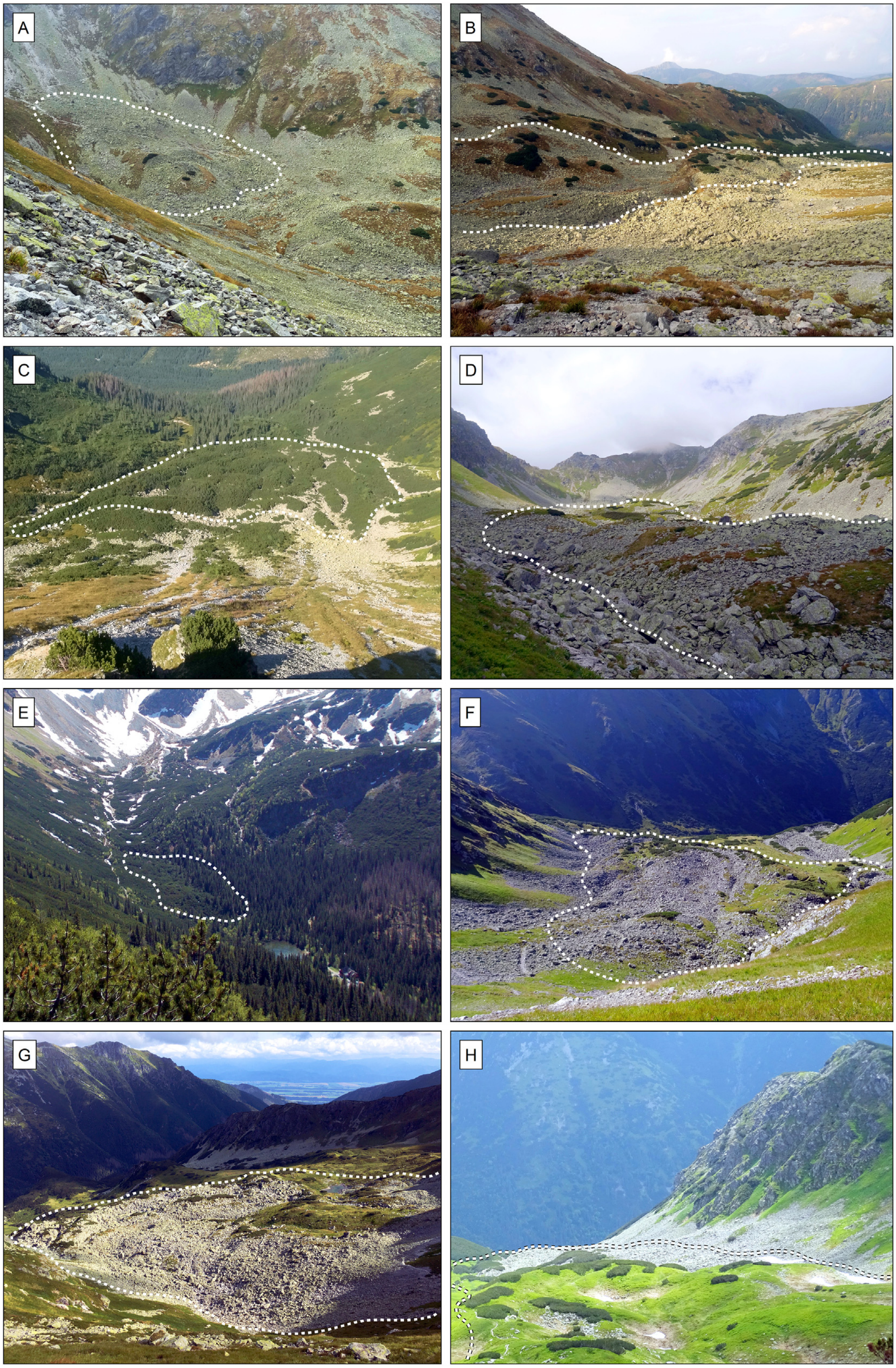

Fig. 2. Rock glaciers selected for exposure dating in the Spálená (A) upper, (B) middle, and (C) lower valley; (D) Smutná valley; (E) Roháčska valley; (F) Žiarska valley; Jamnícka (G) north and (H) south valley. The location of the centroids of the rock glaciers is given in Table 1.

involves isolation and purification of quartz and elimination of atmospheric ^{10}Be. A weighed amount (~0.1 g) of a 3025 ppm solution of ^{9}Be was added to the decontaminated quartz. Beryllium was subsequently separated from the solution by successive anionic and cationic resin extraction and precipitation. The final precipitates were dried and heated at 800 °C to obtain BeO, and finally mixed with niobium powder prior to the measurements, which were performed at the French Accelerator Mass Spectrometry (AMS) National Facility ASTER (CEREGE, Aix-en-Provence).

3.3. ^{10}Be age calculations

The beryllium data were calibrated directly against the STD-11 beryllium standard using a $^{10}Be/^{9}Be$ ratio of $1.191 \pm 0.013 \cdot 10^{-11}$ (Braucher et al., 2015). Age uncertainties include an external AMS uncertainty of 0.5%, blank correction and 1σ uncertainties (Arnold et al., 2010). The $^{10}Be/^{9}Be$ measured blank ratio associated with the samples is $3.618 \cdot 10^{-15}$. A density of 2.5 g cm^{-3} was used for all samples. A sea-level, high-latitude spallation production of 4.01 ± 0.18 at g$^{-1}\cdot$a^{-1} (Borchers et al., 2016) was used and scaled for latitude and elevation using Stone (2000) scaling scheme. The surface production rates were also corrected for the local shielding due to the surrounding terrain (Dunne et al., 1999) and snow cover (Dunai, 2010). The snow covers valley floors in the study area for more than six months per year in the present climate and decreases the cosmogenic nuclides production rate. The present-day data may tentatively represent snow cover in the study area over much of the exposure period as warmer conditions were reported only for short intervals during early and middle Holocene (Kłapyta et al., 2016). Shielding from snow was estimated according to Gosse and Phillips (2001) using an average snow density of 0.3 g cm^{-3} and an estimated mean thickness and duration of snow cover at the sample sites. These values were determined based on the data collected during the period 1960/61–1989/90 at nine weather stations (725–1991 m asl) in the Tatra Mts. (Kočický, 1996).

^{10}Be concentrations were modelled using the equation:

$$C_{(x,\varepsilon,t)} = \frac{P_{spall}}{\frac{\varepsilon}{\Lambda_n} + \lambda} \cdot e^{\frac{-x}{\Lambda_n}} \left[1 - exp\left\{ -t\left(\frac{\varepsilon}{\Lambda_n} + \lambda\right)\right\} \right] + \frac{P_{\mu}}{\frac{\varepsilon}{\Lambda_{\mu}} + \lambda} \cdot e^{\frac{-x}{\Lambda_{\mu}}} \left[1 - exp\left\{ -t\left(\frac{\varepsilon}{\Lambda_{\mu}} + \lambda\right)\right\} \right] \quad (3)$$

where $C_{(x,\varepsilon,t)}$ is the nuclide concentration as a function of depth x (g$\cdot$cm^{-2}), the denudation rate ε (g$\cdot$cm$^{-2}\cdot$a^{-1}), and the exposure time t (a). P_{spall} and P_{μ} (at$\cdot$g$^{-1}\cdot$a^{-1}) are the relative production rates due to neutrons and muons, respectively. Λ_n and Λ_{μ} (g$\cdot$cm^{-2}) are the effective apparent attenuation lengths for neutrons and muons, respectively, and λ (a^{-1}) is the radioactive decay constant. The muon scheme follows Braucher et al. (2011).

Individual ages are reported with an external error of 1σ, which accounts for both measurement uncertainties, including uncertainties associated with AMS counting statistics, chemical blank measurements and AMS internal error (0.5%), as well as uncertainties in the reference nuclide production rate for spallation and the nuclide production rate by muons (Balco et al., 2008). At each site, a weighted mean exposure age was calculated and reported with a weighted mean standard deviation.

The chi-squared (χ^2) test was used to examine the distribution of exposure ages at each site (Ward and Wilson, 1978). The 95% critical value for χ^2 with $n-1$ degrees of freedom was calculated for each site and compared with the theoretical value given by a χ^2 table. If the calculated value was less than the theoretical value, all ages were used to calculate the mean exposure age. However, if the site did not pass this test, the ages with the largest calculated χ^2 value were successively excluded until the distribution passed the χ^2 test (Dunai, 2010). Additionally, the reduced χ^2 statistic (χ^2_R) and the standard deviation to arithmetic mean exposure age ratio was used to approximate the scatter in the data and classify the age groups as well-, moderately- or poorly-clustered (class A, B, and C, respectively) following Blomdin et al. (2016).

4. Results

4.1. Distribution and morphology of rock glaciers

The eight dated rock glaciers occur at an elevation of 1376–1893 m asl (mean 1693 m asl) and their fronts extend to 1376–1819 m asl (mean 1613 m asl) where the present-day MAAT attains 0.2–2.4 °C (mean 1.2 °C, Table 1). Their average length is 591 m, while the average width is 188 m and they occupy an average area of 0.1 km^2. The mean height of the rock glacier fronts is 21 m. Most of the rock glaciers are oriented to the east (four) and northeast (two). The lowermost rock glaciers have predominantly a northeast and northwest orientation. On the contrary, the highest-elevated rock glaciers face east and south. All the rock glaciers are tongue-shaped because the length-to-width ratio is 1.2 (northern Jamnícka valley) to 8.6 (middle Spálená valley, Table 1). Similarly, all the rock glaciers are considered relict because they are prominently covered with vegetation and the mean slope of the fronts ranges between 28° (Roháčska valley) and 33° (Smutná valley).

4.2. ^{10}Be exposure ages

The ^{10}Be exposure ages obtained for the collected samples are given in Table 2 and Fig. 3. Four out of 34 exposure ages are identified as outliers and excluded from the dataset based on the results of the χ^2 test (Table 3). Two outlier ages obtained for the samples SPA-4 and SPA-6 are excluded from the dataset obtained in the

Table 1
Morphometric and climate characteristics of the dated rock glaciers in the Western Tatra Mts.

Rock glacier	Centroid latitude (°N)	Centroid longitude (°E)	Aspect	Minimum elevation (m asl)	Maximum elevation (m asl)	Mean elevation (m asl)	Length of the flowline (m)	Mean width (m)	Area (km^2)	Mean slope (°)	Mean slope of the front (°)	Mean height of the front (m)	Potential incoming solar radiation (W$\cdot$m^{-2})	MAAT at the front (°C)
Jamnícka-North	49.1958	19.7563	E	1745	1845	1798	448	360	0.13	17	32	26	155	0.6
Jamnícka-South	49.1921	19.7582	E	1632	1839	1757	852	129	0.11	17	31	20	147	1.2
Roháčska	49.2113	19.7493	NW	1376	1429	1404	240	192	0.03	18	28	9	129	2.4
Smutná	49.2009	19.7433	E	1564	1824	1713	1106	169	0.16	18	33	20	132	1.5
Spálená-Lower	49.2084	19.7265	NE	1465	1568	1513	366	255	0.09	17	32	18	130	1.9
Spálená-Middle	49.2043	19.7156	NE	1594	1824	1728	1032	120	0.11	19	31	24	135	1.3
Spálená-Upper	49.2022	19.7089	E	1819	1893	1856	192	128	0.02	24	30	22	138	0.2
Žiarska	49.1928	19.7366	S	1706	1855	1778	493	154	0.08	21	32	32	167	0.8

Table 2
^{10}Be surface exposure ages for the samples collected at the rock glaciers in the Western Tatra Mts. Samples with outlier exposure ages are shown in italics.

Rock glacier	Sample	Latitude (°N)	Longitude (°E)	Elevation (m asl)	Thickness (cm)	Length/ width/height (m)	Surface aspect/dip (°)	Snow cover depth/duration (cm/month)	Correction due to snow	Topographic shielding factor	Total shielding correction	Production rate (at·g^{-1}·a^{-1})	^{10}Be concentration (at·g^{-1})	^{10}Be age (ka)
Jamnícka-North	JAM-1	49.19525	19.75797	1779	5	3.3/2.4/1.5	95/7	54/7	0.904	0.977	0.883	16.072	233 477 ± 7263	14.5 ± 0.5
	JAM-2	49.19534	19.75803	1789	4	2.2/2.2/1.7	145/17	55/7	0.902	0.977	0.881	16.155	252 077 ± 8434	15.6 ± 0.5
	JAM-3	49.19557	19.75777	1791	7	4.7/2.3/1.6	310/7	55/7	0.902	0.972	0.877	16.099	212 898 ± 6604	13.2 ± 0.4
	JAM-4	49.19551	19.75779	1785	7	4.5/3.8/3.7	150/5	54/7	0.904	0.975	0.881	16.101	218 539 ± 6740	13.5 ± 0.4
	JAM-5	49.19488	19.75694	1793	4	5.5/1.7/1.4	105/9	55/7	0.902	0.974	0.878	16.151	237 398 ± 7280	14.7 ± 0.5
Jamnícka-South	JAM-6	49.19186	19.76342	1659	2	1.8/1.7/0.6	265/3	49/6	0.912	0.958	0.874	14.542	188 788 ± 8328	13.0 ± 0.6
	JAM-7	49.19178	19.76337	1680	4	2.1/2.0/1.8	75/4	50/6	0.911	0.954	0.868	14.667	188 000 ± 10 620	12.8 ± 0.7
	JAM-8	49.19168	19.76337	1680	3	3.2/2.5/1.4	270/3	50/6	0.911	0.950	0.865	14.616	162 611 ± 9220	11.1 ± 0.6
	JAM-9	*49.19211*	*19.76337*	*1677*	2	0.9/2.7/1.9	horizontal	50/6	0.911	0.953	0.868	14.626	230 485 ± 9388	*15.7 ± 0.6*
Roháčska	ROH-1	49.21115	19.74969	1418	3	3.1/2.4/2.8	horizontal	39/6	0.929	0.945	0.878	12.159	198 833 ± 7044	16.3 ± 0.6
	ROH-2	49.21124	19.74986	1414	4	1.6/1.5/1.3	135/12	39/6	0.929	0.943	0.877	12.097	192 945 ± 10 085	15.9 ± 0.8
	ROH-3	49.21161	19.74991	1412	4	3.4/2.6/1.9	horizontal	39/6	0.929	0.943	0.877	12.070	217 075 ± 15 633	18.2 ± 1.3
	ROH-4	49.21160	19.74983	1409	2	3.2/2.9/2.7	horizontal	39/6	0.929	0.930	0.864	11.879	178 379 ± 10 843	15.5 ± 0.9
Smutná	SMU-1	49.20012	19.74138	1724	3	2.0/1.4/0.75	178/16	52/7	0.907	0.987	0.895	15.637	203 643 ± 6779	13.0 ± 0.4
	SMU-2	49.20020	19.74132	1738	5	2.0/1.5/0.9	105/25	53/7	0.905	0.986	0.893	15.566	177 125 ± 5734	11.4 ± 0.4
	SMU-3	49.20025	19.74030	1752	4	1.9/1.4/0.6	120/15	53/7	0.905	0.989	0.896	15.983	193 222 ± 6376	12.1 ± 0.4
	SMU-4	49.20023	19.74017	1756	6	1.9/1.2/0.8	310/12	53/7	0.905	0.988	0.895	16.010	181 683 ± 5805	11.3 ± 0.4
Spálená-Lower	SPA-1	49.20750	19.72576	1495	3	4.9/4.2/1.5	195/11	42/6	0.924	0.989	0.914	13.982	219 421 ± 9441	16.0 ± 0.7
	SPA-2	49.20745	19.72621	1519	5	4.3/2.9/1.6	190/2	43/6	0.923	0.989	0.912	14.228	239 711 ± 9068	17.5 ± 0.7
	SPA-3	49.20757	19.72588	1530	4	7.1/4.3/2.8	225/9	44/6	0.921	0.989	0.911	14.334	202 145 ± 16 491	14.5 ± 1.2
	SPA-4	*49.20906*	*19.72803*	*1488*	*4*	6.9/6.3/3.3	80/11	42/6	0.924	0.990	*0.915*	*13.922*	*9556 ± 1294*	*0.7 ± 0.1*
	SPA-5	49.20928	19.72791	1487	4	1.9/1.3/1.0	250/7	42/6	0.924	0.992	0.916	13.930	240 855 ± 9728	17.8 ± 0.7
	SPA-6	*49.20930*	*19.72796*	*1490*	*4*	2.2/1.8/1.3	180/23	42/6	0.924	0.992	*0.916*	*13.962*	*149 855 ± 8403*	*11.0 ± 0.6*
Spálená-Middle	SPA-10	49.20386	19.71408	1753	5	7.9/5.7/4.0	270/7	53/7	0.905	0.989	0.895	16.680	287 144 ± 16 600	17.9 ± 1.0
	SPA-11	49.20390	19.71405	1752	3	6.7/4.6/2.2	25/6	53/7	0.905	0.989	0.895	16.667	337 747 ± 23 703	20.7 ± 1.5
	SPA-12	49.20451	19.71537	1730	5	8.7/6.3/4.7	285/8	52/7	0.907	0.990	0.898	16.436	260 480 ± 9998	16.5 ± 0.6
Spálená-Upper	SPA-7	49.20210	19.70855	1867	3	4.7/3.3/1.5	60/16	58/7	0.897	0.982	0.881	18.090	244 564 ± 9158	13.8 ± 0.5
	SPA-8	49.20228	19.70846	1870	3	3.8/2.6/1.8	185/5	58/7	0.897	0.979	0.878	17.909	233 403 ± 9086	13.3 ± 0.5
	SPA-9	*49.20232*	*19.70868*	*1865*	*4*	3.0/2.8/1.5	horizontal	58/7	0.897	0.981	*0.880*	*17.884*	*361 949 ± 22 357*	*20.9 ± 1.3*
Žiarska	ZIA-1	49.19293	19.73539	1778	4	2.0/1.4/0.8	205/8	54/7	0.904	0.958	0.865	15.741	240 364 ± 7635	15.2 ± 0.5
	ZIA-2	49.19276	19.73560	1779	5	2.6/2.0/1.1	25/12	54/7	0.904	0.963	0.870	15.837	224 922 ± 6970	14.2 ± 0.4
	ZIA-3	49.19279	19.73671	1775	4	4.9/3.0/1.0	150/4	54/7	0.904	0.948	0.857	15.554	210 529 ± 6489	13.5 ± 0.4
	ZIA-4	49.19251	19.73682	1776	5	2.7/1.9/1.9	15/19	54/7	0.904	0.959	0.866	15.731	233 125 ± 8078	14.8 ± 0.5
	ZIA-5	49.19260	19.73613	1774	6	1.9/1.8/1.3	215/6	54/7	0.904	0.961	0.869	15.587	258 651 ± 8015	16.6 ± 0.5

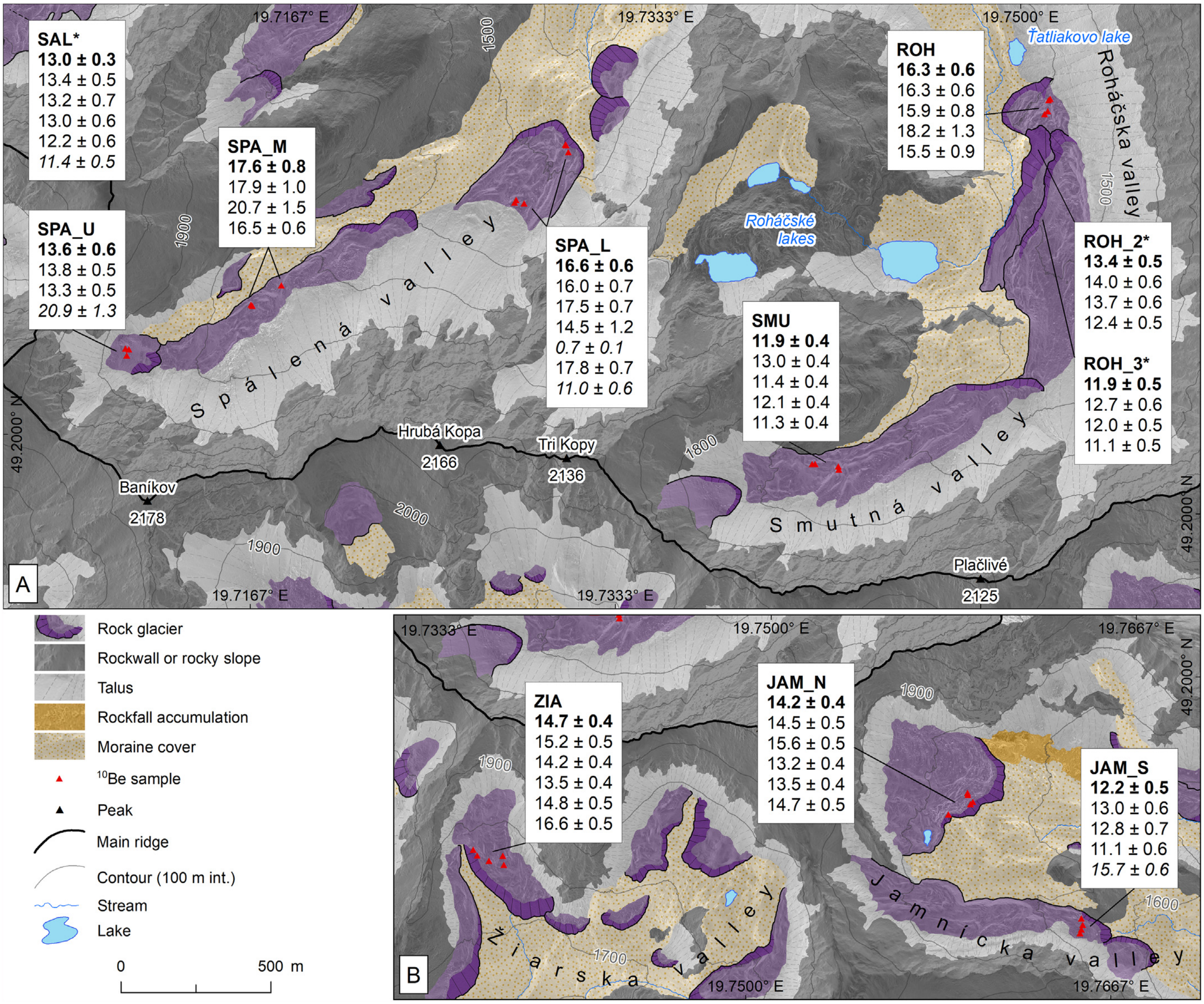

Fig. 3. ^{10}Be exposure ages for the sampled boulders and weighted mean exposure ages (bold) for the dated rock glaciers in the Western Tatra Mts. Italics indicates exposure ages removed from the dataset based on the χ^2 test. Asterisks represent dates published by Engel et al. (2017). Geomorphological features follow Kłapyta (2015). The location of the centroids of the dated rock glaciers and individual samples is given in Tables 1 and 2, respectively.

Table 3
^{10}Be surface exposure ages for the sampled rock glaciers in the Western Tatra Mts. The location of the rock glacier centroids and individual samples is given in Tables 1 and 2, respectively.

Rock glacier	Number of samples/ sample code	Theoretical χ^2	χ^2	χ^2_R	SD to arithmetic mean exposure age (%)	Age clustering (class)[a]	Uncertainty-weighted mean age ± Uncertainty (ka)	Arithmetic mean age ± Uncertainty (ka)
Jamnícka-North	5/JAM-1 to JAM-5	9.49	5.03	1.3	7	A	14.2 ± 0.4	14.3 ± 0.4
Jamnícka-South	3/JAM-6 to JAM-8	5.99	2.88	1.4	8	A	12.2 ± 0.5	12.3 ± 0.6
Roháčska	4/ROH-1 to ROH -4	7.81	2.18	0.7	7	A	16.3 ± 0.6	16.5 ± 0.6
Smutná	4/SMU-1 to SMU-4	7.81	3.46	1.2	7	A	11.9 ± 0.4	11.9 ± 0.4
Spálená-Lower	4/SPA-1 to SPA-3, SPA-5	7.81	4.39	1.5	9	A	16.6 ± 0.6	16.5 ± 0.8
Spálená-Middle	3/SPA-10 to SPA-12	5.99	5.27	2.6	12	B	17.6 ± 0.8	18.4 ± 1.3
Spálená-Upper	2/SPA-7 to SPA-8	3.84	0.17	0.2	3	A	13.6 ± 0.6	13.6 ± 0.3
Žiarska	5/ZIA-1 to ZIA-5	9.49	6.85	1.7	8	A	14.7 ± 0.4	14.9 ± 0.5

[a] The degree of scatter in ages according to the method of Blomdin et al. (2016).

lower part of the Spálená valley. The remaining four exposure ages range from 17.8 ± 0.7 ka to 14.5 ± 1.2 ka and yield a weighted mean exposure age of 16.6 ± 0.6 ka. At the Spálená valley head closure, the sample SPA-9 with an exposure age of 20.9 ± 1.3 ka is identified as an outlier and excluded from the mean exposure age calculation for the site. The remaining two samples yield a weighted mean exposure age of 13.6 ± 0.6 ka. The last outlier age of the sample JAM-9 is identified in the set of samples from the southern rock glacier in the Jamnícka valley. The remaining three exposure ages range from 11.1 ± 0.6 ka to 13.0 ± 0.6 ka and give a weighted mean exposure age of 12.2 ± 0.5 ka.

The dispersion of the exposure ages is rather limited for the rock glaciers in the Roháčska and Smutná valleys (Fig. 3). The four ages obtained in the Roháčska valley are well-clustered between 18.2 ± 1.3 ka and 15.5 ± 0.9 ka, yielding a weighted mean age of 16.3 ± 0.6 ka. Similarly, ages obtained for four samples collected in the Smutná valley are well-clustered between 13.0 ± 0.4 ka and 11.3 ± 0.4 ka, giving a weighted mean age of 11.9 ± 0.4 ka. Well-clustered exposure ages were also obtained for five samples collected from the northern rock glacier in the Jamnícka valley. These ages range from 15.6 ± 0.5 ka to 13.2 ± 0.4 ka and give a weighted mean exposure age of 14.2 ± 0.4 ka. Five samples collected in the Žiarska valley yield well-clustered ages between 16.6 ± 0.5 ka and 13.5 ± 0.4 ka giving a weighted mean exposure age of 14.7 ± 0.4 ka. The three exposure ages obtained for the rock glacier in the middle part of the Spálená valley are moderately-clustered between 20.8 ± 1.5 ka and 16.5 ± 0.6 ka, with a weighted mean age of 17.6 ± 0.8 ka.

5. Discussion

5.1. Age of rock glaciers

The dated rock glaciers in cirques, middle sections of troughs, and their lower portions above the transition to main valleys represent a complete set of locations where these landforms were found in the Western Tatra Mts. (Uxa and Mida, 2017). The mean elevation of their fronts is only ~30 m lower compared to that reported for all rock glaciers in the Western Tatra Mts. and the dated rock glacier in the Roháčska valley belongs to the lowermost in the mountain range (Uxa and Mida, 2017). Consequently, we believe that the dated rock glaciers are representative of the whole Western Tatra Mts.

The cosmogenic nuclide ages imply that rock glaciers in the Western Tatra Mts. started to form after the retreat of local glaciers from their LGM positions. The absence of outlier ages in the sample set from the oldest dated rock glacier in the middle Spálená valley suggests that this feature formed after ~18 ka. However, moderately clustered ages indicate movements of individual sampled boulders implying that this rock glacier was ice-cored and active until ~16.5 ka. At that time, glaciers in cirques and tributary valleys were separated from the glacier in the main trough as evidenced by exposure ages reported for the Roháčské lakes area (Engel et al., 2017). The coincident uncertainty-weighted mean ages obtained for the rock glaciers in the lower Spálená (16.6 ± 0.6 ka) and Roháčska (16.3 ± 0.6 ka) valleys suggest that these forms probably evolved from the material of retreating glaciers during the GS-2.1a (17.5–14.7 ka; Rasmussen et al., 2014). Later rock glacier stabilization cannot be excluded at the lower Spálená site based on the presence of younger ages in the dataset.

The mean ages calculated for the rock glaciers in the Žiarska, northern Jamnícka, and upper Spálená valleys fall in the Lateglacial interstadial GI-1 (14.7–12.9 ka; Rasmussen et al., 2014). Paleoenvironmental proxies in peat and lake sediments indicate continental climate throughout this period with relatively warm summer months until 12.9 ka (Obidowicz, 1996; Rybníčková and Rybníček, 2006). Older mean ages (14.7 ± 0.4 and 14.2 ± 0.4 ka) obtained for the rock glaciers in the southern mountain flank may be attributed to earlier glacier retreat due to the higher potential incoming solar radiation and temperature compared to the upper Spálená rock glacier (13.6 ± 0.6 ka) at higher-elevated site with NE aspect (Table 1). The youngest exposure ages obtained for these rock glaciers indicate their final stabilization within relatively short period (13.5–13.2 ka) at the end of the interstadial.

The dated rock glaciers in the southern Jamnícka and Smutná valleys have an eastern orientation similarly to the northern Jamnícka rock glacier, but their surface is shaded by the adjacent mountain ridges as evidenced by the lower beam radiation (Table 1). As a result, glacier snouts melted slowly, and the successive rock glaciers formed as late as in the GS-1 (12.2 ± 0.5 and 11.9 ± 0.4 ka). The youngest exposure ages retrieved for the southern Jamnícka site, as well as a pair of almost identical youngest ages collected in the Smutná valley (Fig. 3) suggest that the rock glaciers at these sites became inactive around 11.3 ± 0.4 ka. This timing coincides with the mean exposure age of 11.1 ± 0.9 ka retrieved for high-elevated rock glaciers in the SW part of the High Tatra Mts., but predates the final stabilization of these landforms around 10.4 ka (Zasadni et al., 2020).

The timing of the rock glacier activity in the Western Tatra Mts. between ~18 and 11 ka (Fig. 4) is consistent with the major period of development of these landforms in other European mountain ranges. In accordance with local glaciation chronologies, the rock glacier stabilization in the Western Tatra Mts. (16.5–11 ka) took place around the same time as in the mountain ranges on the Iberian Peninsula (15.7–11.5 ka) but earlier than in the Alps (12.4–9.6 ka). The main phase of rock glacier stabilization overlaps with the GS-1 period, similarly as in the High Tatra Mts. (Zasadni et al., 2020), Alps (Moran et al., 2016; Charton et al., 2021), or Sierra Nevada (Palacios et al., 2016). The stabilization of rock glaciers in the mainland Europe terminated during the onset of the Holocene in the Tatra Mts (Zasadni et al., 2020). and Alps (Ivy-Ochs and Schaller, 2009; Charton et al., 2021), while lasted until the mid-Holocene period in the Pyrenes (Andrés et al., 2018), Sierra Nevada (Palacios et al., 2016) and Tröllaskagi Peninsula, Iceland (Palacios et al., 2021).

5.2. Paleoclimatic and paleopermafrost implications

A minimum temperature declines relative to the present MAAT derived for the three oldest rock glaciers from the GS-2.1 is −3.9 °C and their fronts at ~1480 m asl are ~840 m lower compared to the present lower limit of discontinuous permafrost. These changes are close to the MAAT and elevation decrease of −3.7 to −3 °C and ~630–770 m, respectively, reported for the GS-2.1 rock glaciers in the High Tatra Mts. (Zasadni et al., 2020). On the other hand, these MAAT declines are much smaller than −10 to −9 °C derived for the GS-2.1 based on glacier modelling in the High Tatra Mts. (Makos et al., 2013, 2018). Similarly, the relevance of the GS-2.1 rock glaciers for the lower limit of discontinuous permafrost is also unclear because it is inconsistent with other local and regional paleopermafrost features (Fig. 5). Cryogenic-carbonate deposits found in caves in the High and Low Tatra Mts. indicate the presence of permafrost at ~670 m asl between ~17.1 ± 0.1 ka and ~15.2 ± 0.6 ka (Žák et al., 2012; Orvošová et al., 2014). Besides that, there is extensive evidence for at least discontinuous permafrost in the nearby Central European lowlands <~250 m asl as far south as 47°N between 18.1 ± 0.4 ka and 14.8 ± 0.1 ka based on the occurrence of relict frost wedges (Kovács et al., 2007; Fiedorczuk et al., 2007; Fábián et al., 2014; Ewertowski et al., 2017; Farkas et al., 2023) and pingo scars (Hošek et al., 2020). This implies that permafrost was ubiquitous in the GS-2.1 and not limited to mountain areas. Considering the elevation of the lowermost GS-2.1 permafrost features in the Tatra Mts. and the nearby Central European lowlands of ~670 and ~60 m asl, respectively (Fig. 5), the MAAT decline

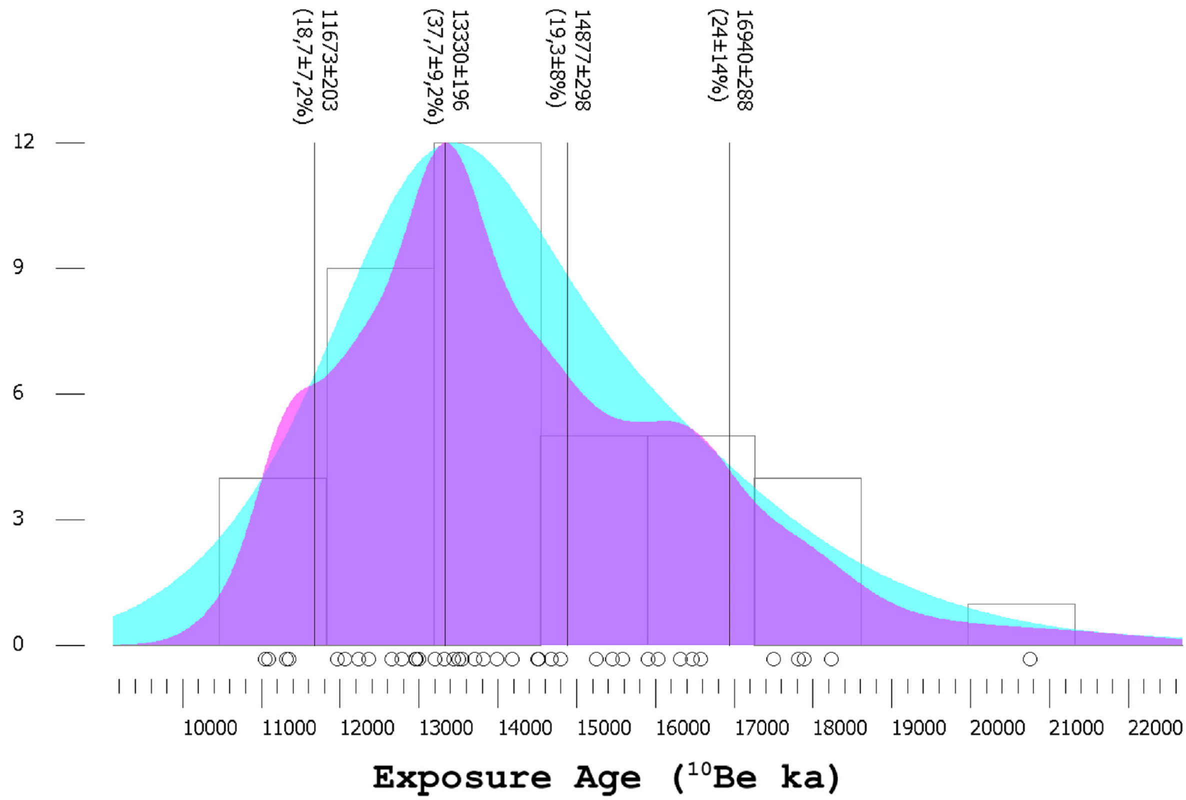

Fig. 4. Timing of rock glacier stabilization in the Western Tatra Mts. The probability density plot (purple shading) and Kernel Density Estimation (in cyan) of ^{10}Be exposure ages (n = 40) obtained in this study and reported for rock glaciers in the Roháčska and Salatínska valleys by Engel et al. (2017). Vertical lines indicate mean ages with proportions for the modelled peaks and open circles show individual exposure ages (Vermeesch, 2012).

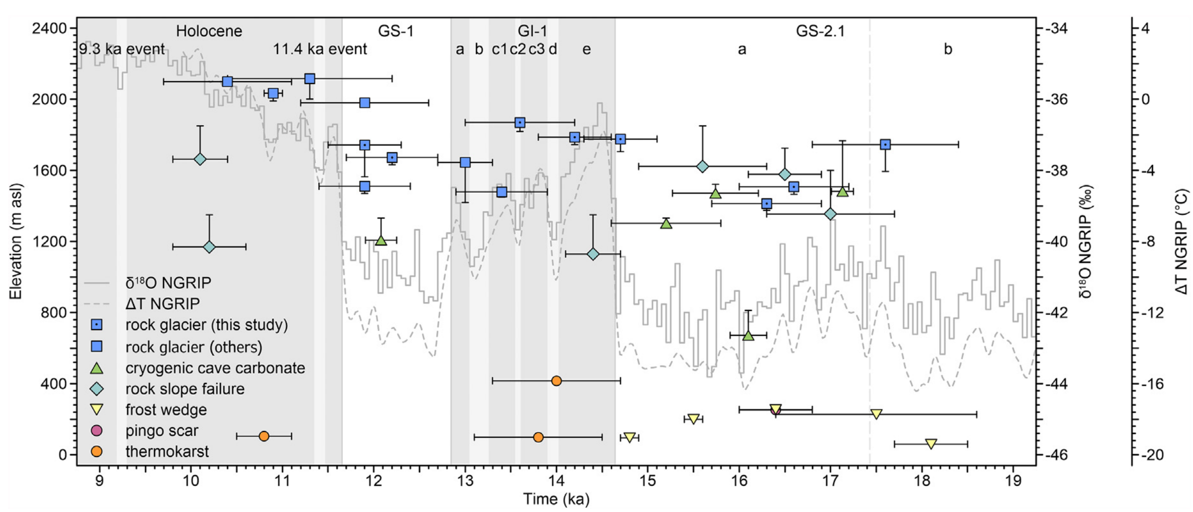

Fig. 5. Timing of rock glaciers and other paleopermafrost features around the Tatra Mts. Exposure ages for rock glaciers after Engel et al. (2017), Zasadni et al. (2020), and this study. Cryogenic cave carbonates (Žák et al., 2012; Orvošová et al., 2014), rock slope failures (Pánek et al., 2016), frost wedges (Kovács et al., 2007; Fiedorczuk et al., 2007; Fábián et al., 2014; Ewertowski et al., 2017; Farkas et al., 2023), pingo scar (Hošek et al., 2020), and thermokarst features (Błaszkiewicz, 2011; Błaszkiewicz et al., 2015; Hošek et al., 2019) constrain the timing of permafrost occurrence or permafrost degradation. The weighted mean ages and weighted mean standard deviations for individual locations are reported. Vertical bars show the elevation of rock glacier fronts, entrance of caves, and the lowest detachment zone for rock slope failures. The temperature offset (grey dashed line) relative to the present (Kindler et al., 2014), δ^{18}O data (grey solid line), and INTIMATE event stratigraphy (Rasmussen et al., 2014) are derived from the NGRIP ice core on the GICC05modelext time scale.

in the GS-2.1 attains −7.7 °C and −10.5 °C, respectively. This is much closer to the MAAT decline reported by Makos et al. (2013, 2018) for the High Tatra Mts., as well as to the temperature decline of < −11 °C indicated by the lowland permafrost features (*sensu* Huijzer and Isarin, 1997; Huijzer and Vandenberghe, 1998). The plausibility of the larger MAAT decline also reflects the maximum elevation of the GS-2.1 rock glaciers (~rock glacier initiation altitude) of ~1610 m asl that fits the paleo-equilibrium line altitude at 1600−1700 m asl modelled in the High Tatra Mts. (Makos et al., 2013, 2018), as these two elevation indices are generally assumed to closely correspond (Humlum, 1998).

The three rock glaciers attributed to the GI-1 indicate a minimum MAAT decline of −2.5 °C and their fronts at ~1760 m asl suggest a decrease of the lower limit of discontinuous permafrost by ~560 m relative to the present. Engel et al. (2017) dated other two GI-1 rock glaciers in the study area at ~1440 m, which correspond to a MAAT decline of −4.1 °C and a decrease of the lower limit of discontinuous permafrost by ~880 m. These values seem reasonable because no other paleopermafrost features are present at lower elevations (Fig. 5) and there was a rapid climate warming at the onset of the GI-1 (Kindler et al., 2014), which prompted the thermokarst development in the nearby Central European lowlands between ~14.0 ± 0.7 cal ka and ~13.8 ± 0.7 cal ka (Błaszkiewicz, 2011; Błaszkiewicz et al., 2015; Hošek et al., 2019). Permafrost degradation may also have triggered a rock slope failure that initiated >1350 m asl at 14.4 ± 0.3 ka in the Western Tatra Mts. (Pánek et al., 2016). As rock glaciers tend to move faster with higher temperatures (Kääb et al., 2007), the warmer climate of the GI-1 may have enhanced the rock glacier activity (Fig. 4), which could have been further promoted by a possible higher debris supply from collapsing slopes.

The two GS-1 rock glaciers suggest a MAAT decline of −3.4 °C and their fronts at ~1600 m asl correspond to a decrease of the lower limit of discontinuous permafrost by ~720 m. These indices differ from the values of −1.6 °C, ~2030 m asl, and ~335 m, respectively, reported by Zasadni et al. (2020) for rock glaciers in the High Tatra Mts. Nevertheless, there is another GS-1 rock glacier in the study area at ~1470 m asl (Engel et al., 2017) and a cryogenic-carbonate deposit in the Low Tatra Mts. further suggests that permafrost descended to at least ~1210 m asl 12.1 ± 0.2 ka (Fig. 5) (Orvošová et al., 2014), which implies a MAAT decline of at least −5.2 °C. This is plausible because the maximum elevation of the GS-1 rock glaciers of ~1830 m asl is just below the paleo-equilibrium line altitude at 1900 m asl modelled for the MAAT decline of −7 to −6 °C in the High Tatra Mts. (Makos et al., 2013, 2018). At the same time, it is consistent with the assumptions that only seasonally frozen ground existed in the nearby Central European lowlands south of 50°N in the GS-1 (Isarin, 1997), and isolated islands of permafrost occurred only in high mountain areas.

The aforementioned discrepancies between the lower limit of the rock glaciers and other paleopermafrost features in the GS-2.1 and GS-1 (Fig. 5) may result from topographic constraints, limited debris supply, unfavourable climatic conditions and/or insufficient time for development of the rock glaciers (Barsch, 1996; Kääb, 2013). Alternatively, they may reflect glacial rather than permafrost origin of the rock glaciers (Whalley and Martin, 1992; Jones et al., 2019), which is also supported by the fact that their maximum elevations correspond well with the paleo-equilibrium line altitudes (Makos et al., 2013, 2018). Whatever the reason, the rock glaciers in the Western Tatra Mts. seem to underestimate past permafrost extents and temperature declines and should be used cautiously as paleoenvironmental proxies.

Since the beginning of the Holocene, climate warmed and permafrost degraded, which resulted in the final stabilization of the youngest rock glaciers at 1564–1632 m asl around 11.3 ± 0.4 ka. The increasing ground temperatures conditioned slope instability initiating rock slope failures >1850 m asl in the Western Tatra Mts. 10.2 ± 0.4 ka and 10.1 ± 0.3 ka (Pánek et al., 2016). The timing of the rapid permafrost degradation is consistent with the peak of the thermokarst activity in northern Poland at ~10.8 ± 0.3 cal ka (Błaszkiewicz, 2011; Błaszkiewicz et al., 2015).

6. Conclusions

The dataset of ^{10}Be exposure ages obtained for rock glaciers in the Western Tatra Mts., Western Carpathians, documents their activity between ~18 and 11 ka. This activity is attributed to three main phases: (1) 17.6 ± 0.8 to 16.3 ± 0.6 ka, (2) 14.7 ± 0.4 to 13.6 ± 0.6 ka, and (3) 12.2 ± 0.5 to 11.9 ± 0.4 ka. The oldest dated rock glaciers with front elevation of 1376–1594 m asl started to form during the Greenland Stadial 2.1 following the retreat of glaciers from their LGM positions. The middle phase of activity reflects warm conditions during the Greenland Interstadial 1 and the youngest landforms coincide with the Greenland Stadial 1 (~Younger Dryas). The final stabilization of the youngest rock glaciers with fronts located at an elevation of 1564–1632 m asl probably lasted until the beginning of the Holocene as indicate exposure ages of 11.3 ± 0.4 and 11.1 ± 0.6 ka obtained for boulders at the northern foot of the main mountain ridge.

The initiation altitude of ~1610 and 1830 m asl determined for the rock glaciers from the Greenland Stadials 2.1 and 1, respectively, is consistent with estimates of the paleo-equilibrium line altitude reported for these periods. By contrast, the lower limit of the rock glaciers is well above other regional paleopermafrost features from the same periods. This suggests that elevation indices derived for the rock glaciers in the Western Tatra Mts. underestimate past permafrost extents and temperature declines raising questions about their validity for paleoenvironmental reconstructions. The closer relation of these indices to paleo-equilibrium line altitude suggests a glacial rather than periglacial origin of the dated rock glaciers.

Funding

This research was supported by the Charles University Grant Agency (project no. 1528119) and the Czech Science Foundation (project 21-23196S). ASTER AMS national facility (CEREGE, Aix-en-Provence, France) is supported by the INSU/CNRS, and IRD.

CRediT authorship contribution statement

Tereza Dlabáčková: Conceptualization, Methodology, Formal analysis, Investigation, Writing – original draft, Visualization, Funding acquisition. **Zbyněk Engel:** Conceptualization, Methodology, Formal analysis, Investigation, Writing – original draft, Visualization, Supervision. **Tomáš Uxa:** Conceptualization, Methodology, Formal analysis, Investigation, Writing – original draft, Visualization. **Régis Braucher:** Investigation, Writing – review & editing. **Aster Team:** Investigation.

Declaration of competing interest

The authors declare that they have no known competing financial interests or personal relationships that could have appeared to influence the work reported in this paper.

Data availability

Data will be made available on request.

Acknowledgements

The Tatra National Park Administration is thanked for providing permission to work in the protected area. The authors thank Shaun Eaves and an anonymous reviewer for their helpful comments on the manuscript.

References

Andrés, N., Gómez-Ortiz, A., Fernández-Fernández, J.M., Tanarro, L.M., Salvador-Franch, F., Oliva, M., Palacios, D., 2018. Timing of deglaciation and rock glacier

origin in the southeastern Pyrenees: a review and new data. Boreas 47 (4), 1050–1071. https://doi.org/10.1111/bor.12324.
Arnold, M., Merchel, S., Bourlès, D.L., Braucher, R., Benedetti, L., Finkel, R.C., Aumaître, G., Gottdang, A., Klein, M., 2010. The French accelerator mass spectrometry facility ASTER: improved performance and developments. Nucl. Instrum. Methods Phys. Res., Sect. B 268, 1954–1959. https://10.1016/j.nimb.2010.02.107.
Balco, G., Stone, J.O., Lifton, N.A., Dunai, T.J., 2008. A complete and easily accessible means of calculation surface exposure ages or erosion rates from ^{10}Be and ^{26}Al measurements. Quat. Geochronol. 3, 174–195. https://doi.org/10.1016/j.quageo.2007.12.001.
Ballantyne, C.K., Schnabel, C., Xu, S., 2009. Exposure dating and reinterpretation of coarse debris accumulations ('rock glaciers') in the Cairngorm Mountains, Scotland. J. Quat. Sci. 24 (1), 19–31. https://doi.org/10.1002/jqs.1189.
Ballantyne, C.K., 2018. Periglacial Geomorphology. Wiley-Blackwell, Hoboken.
Barsch, D., 1996. Rockglaciers: Indicators for the Present and Former Geoecology in High Mountain Environments, vol. 16. Springer Science & Business Media, Berlin Heidelberg.
Baumgart-Kotarba, M., Král̆, J., 2002. Young tectonic uplift of the Tatra Mts (Fission track data and geomorphological arguments). In: Proceedings of XVII. Congress of Carpathian-Balkan Geological Association. Geol. Carpathica, 53, Special Issue – CD with Extended Abstracts.
Błaszkiewicz, M., 2011. Timing of the final disappearance of permafrost in the central European Lowland, as reconstructed from the evolution of lakes in N Poland. Geol. Q. 55, 361–374.
Błaszkiewicz, M., Piotrowski, J.A., Brauer, A., Gierszewski, P., Kordowski, J., Kramkowski, M., Lamparski, P., Lorenz, S., Noryśkiewicz, A.M., Ott, F., Słowiński, M., Tyszkowski, S., 2015. Climatic and morphological controls on diachronous postglacial lake and river valley evolution in the area of Last Glaciation, northern Poland. Quat. Sci. Rev. 109, 13–27. https://doi.org/10.1016/j.quascirev.2014.11.023.
Blomdin, R., Stroeven, A.P., Harbor, J.M., Lifton, N.A., Heyman, J., Gribenski, N., Petrakov, D.A., Caffee, M.W., Ivanov, M.N., Hättestrand, C., Rogozhina, I., Usubaliev, R., 2016. Evaluating the timing of former glacier expansions in the Tian Shan: a key step towards robust spatial correlations. Quat. Sci. Rev. 153, 78–96. https://10.1016/j.quascirev.2016.07.029.
Böhlert, R., Compeer, M., Egli, M., Brandová, D., Maisch, M., Kubik, P.W., Haeberli, W., 2011. A combination of relative-numerical dating methods indicates two high Alpine rock glacier activity phases after the glacier advance of the Younger Dryas. Open Geogr. J. (4), 115–130. https://doi.org/10.2174/1874923201104010115.
Borchers, B., Marrero, S., Balco, G., Caffee, M., Goehring, B., Lifton, N., Nishiizumi, K., Phillips, F., Schaefer, J., Stone, J., 2016. Geological calibration of spallation production rates in the CRONUS-Earth project. Quat. Geochronol. 31, 188–198. https://doi:10.1016/j.quageo.2015.01.009.
Braucher, R., Merchel, S., Borgomano, J., Bourlès, D.L., 2011. Production of cosmogenic radionuclides at great depth: a multi element approach. Earth Planet Sci. Lett. 309 (1–2), 1–9. https://doi:10.1016/j.epsl.2011.06.036.
Braucher, R., Guillou, V., Bourlès, D.L., Arnold, M., Aumaître, G., Keddadouche, K., Nottoli, E., 2015. Preparation of ASTER in-house ^{10}Be/^{9}Be standard solutions. Nucl. Instrum. Methods Phys. Res. B 361, 335–340. https://doi.org/10.1016/j.nimb.2015.06.012.
Charton, J., Verfaillie, D., Jomelli, V., Francou, B., ASTER Team., 2021. Early Holocene rock glacier stabilisation at col du Lautaret (French Alps): palaeoclimatic implications. Geomorphology 394, 107962. https://doi.org/10.1016/j.geomorph.2021.107962.
Chmeleff, J., von Blanckenburg, F., Kossert, K., Jakob, D., 2010. Determination of the ^{10}Be half-life by multicollector ICP-MS and liquid scintillation counting. Nucl. Instrum. Methods Phys. Res. B 263 (2), 192–199. https://doi.org/10.1016/j.nimb.2009.09.012.
Colucci, R.R., Boccali, C., Žebre, M., Guglielmin, M., 2016. Rock glaciers, protalus ramparts and pronival ramparts in the south-eastern Alps. Geomorphology 269, 112–121. https://doi.org/10.1016/j.geomorph.2016.06.039.
Denn, A.R., Bierman, P.R., Zimmerman, S.R.H., Caffee, M.W., Corbett, L.B., Kirby, E., 2018. Cosmogenic nuclides indicate that boulder fields are dynamic, ancient, multigenerational features. GSA Today (Geol. Soc. Am.) 28, 4–10. https://doi.org/10.1130/GSATG340A.1.
Dlabáčková, T., Engel, Z., 2022. Rainfall thresholds of the 2014 Smutná valley debris flow in western Tatra mountains, Carpathians, Slovakia. Acta Univ. Carol. Geograph. 57 (1), 3–15. https://doi.org/10.14712/23361980.2022.1.
Dobiński, W., 2005. Permafrost of the carpathian and balkan mountains, eastern and southeastern Europe. Permafrost Periglac 16 (4), 395–398. https://doi.org/10.1002/ppp.524.
Dunai, T.J., 2010. Cosmogenic Nuclides – Principles, Concepts and Applications in the Earth Surface Sciences. Cambridge University Press, New York.
Dunne, J., Elmore, D., Muzikar, P., 1999. Scaling factors for the rates of production of cosmogenic nuclides for geometric shielding and attenuation at depth on sloped surfaces. Geomorphology 27 (1–2), 3–11. https://doi:10.1016/S0169-555X(98)00086-5.
Engel, Z., Mentlík, P., Braucher, R., Křížek, M., Pluháčková, ASTER Team, 2017. ^{10}Be exposure age chronology of the last glaciation of the Roháčska Valley in the Western Tatra Mountains, central Europe. Geomorphology 293, 130–142. https://doi.org/10.1016/j.geomorph.2017.05.012.
Ewertowski, M.W., Kijowski, A., Szuman, I., Tomczyk, A.M., Kasprzak, L., 2017. Low-altitude remote sensing and GIS-based analysis of cropmarks: classification of past thermal-contraction-crack polygons in central western Poland. Geomorphology 293, 418–432. https://doi.org/10.1016/j.geomorph.2016.07.022.
Fábián, S.Á., Kovács, J., Varga, G., Sipos, G., Horváth, Z., Thamó-Bozsó, E., Tóth, G., 2014. Distribution of relict permafrost features in the Pannonian Basin, Hungary. Boreas 43, 722–732. https://doi.org/10.1111/bor.12046.
Farkas, B., Sipos, G., Bartyik, T., Józsa, E., Czigány, S., Balogh, R., Varga, G., Kovács, J., Fábián, S.A., 2023. Characterization and mapping of MIS-2 thermal contraction crack polygons in Western Transdanubia, Hungary. Permafrost Periglac 1–11. https://doi.org/10.1002/ppp.2190.
Fernández-Fernández, J.M., Palacios, D., Andrés, N., Schimmelpfennig, I., Tanarro, L.M., Brynjólfsson, López-Acevedo, F.J., Sæmundsson, Þ., ASTER Team., 2020. Constraints on the timing of debris-covered and rock glaciers: an exploratory case study in the Hólar area, northern Iceland. Geomorphology 361, 107196. https://doi.org/10.1016/j.geomorph.2020.107196.
Fiedorczuk, J., Bratlund, B., Kolstrup, E., Schild, R., 2007. Late Magdalenian feminine flint plaquettes from Poland. Antiquity 81, 97–105. https://doi.org/10.1017/S0003598X00094862.
Frauenfelder, R., Haeberli, W., Hoelzle, M., Maisch, M., 2001. Using relict rockglaciers in GIS-based modelling to reconstruct Younger Dryas permafrost distribution patterns in the Err-Julier area. Swiss Alp. Nor. Geogr. Tidsskr. 55 (4), 195–202. https://doi.org/10.1080/00291950152746522.
Frauenfelder, R., Laustela, M., Kääb, A., 2005. Relative age dating of Alpine rockglacier surfaces. Z. Geomorphol. 49 (2), 145–166.
French, H.M., 2017. The Periglacial Environment, fourth ed. Wiley, Chichester.
Gądek, B., 2011. Wieloletnia zmienność kriosfery Tatr. Czasopismo Geograficzne 82 (4), 371–385.
Gądek, B., 2014. Climatic sensitivity of the non-glaciated mountains cryosphere (Tatra Mts., Poland and Slovakia). Global Planet. Change 121, 1–8. https://doi.org/10.1016/j.gloplacha.2014.07.001.
García-Ruiz, J.M., Palacios, D., Fernández-Fernández, J.M., Andrés, N., Arnáez, J., Gómez-Villar, A., Santos-González, J., Álvarez-Martínez, J., Lana-Renault, N., Léanni, L., ASTER Team, 2020. Glacial stages in the Peña Negra valley, Iberian Range, northern Iberian Peninsula: assessing the importance of the glacial record in small cirques in a marginal mountain area. Geomorphology 362, 107195. https://doi.org/10.1016/j.geomorph.2020.107195.
GKÚ Bratislava, N.L.C., 2021. Orthophotomosaic of the Slovak Republic. Geodetic and Cartographic Institute, Bratislava.
Gosse, J.C., Phillips, F.M., 2001. Terrestrial in situ cosmogenic nuclides: theory and application. Quat. Sci. Rev. 20, 1475–1560. https://doi:10.1016/S0277-3791(00)00171-2y.
Haeberli, W., King, L., Flotron, A., 1979. Surface movement and lichen cover studies at the active rock glacier near the Grubengletscher, Wallis, Swiss Alps. Arctic Antarct. Alpine Res. 11 (4), 421–441.
Haeberli, W., 1985. Creep of mountain permafrost: internal structure and flow of alpine rock glaciers. Mit. Ver. Wass. 77, 1–142.
Hamilton, S.J., Whalley, W.B., 1995. Preliminary results from the lichenometric study of the Nautardálur rock glacier, Tröllaskagi, northern Iceland. Geomorphology 12 (2), 123–132. https://doi.org/10.1016/0169-555X(94)00083-4.
Hippolyte, J.C., Bourlès, D., Braucher, R., Carcaillet, J., Léanni, I., Arnold, M., Aumaitre, G., 2009. Cosmogenic ^{10}Be dating of a sackung and its faulted rock glaciers, in the Alps of Savoy (France). Geomorphology 108 (3–4), 312–320. https://doi.org/10.1016/j.geomorph.2022.108112.
Hošek, J., Prach, J., Křížek, M., Šída, P., Moska, P., Pokorný, P., 2019. Buried late weichselian thermokarst landscape discovered in the Czech republic, central Europe. Boreas 48, 988–1005. https://doi.org/10.1111/bor.12404.
Hošek, J., Radoměřský, T., Křížek, M., 2020. Pozdně glaciální termokrasové jevy na severním okraji víděňské pánve (Late Glacial thermokarst phenomena on the northern margin of the Vienna Basin (Czech Republic) (in Czech). Geosci. Res. Rep. 53, 65–72. https://doi.org/10.3140/zpravy.geol.2020.42.
Huijzer, A.S., Isarin, R.F.B., 1997. The reconstruction of past climates using multi-proxy evidence: an example of the weichselian pleniglacial in northwest and central Europe. Quat. Sci. Rev. 16, 513–533. https://doi.org/10.1016/S0277-3791(96)00080-7.
Huijzer, B., Vandenberghe, J., 1998. Climatic reconstruction of the weichselian pleniglacial in northwestern and central Europe. J. Quat. Sci. 13, 391–417. https://doi.org/10.1002/(SICI)1099-1417(1998090)13:5<391::AID-JQS397>3.0.CO;2-6.
Humlum, O., 1998. The climatic significance of rock glaciers. Permafrost Periglac 9, 375–395. https://doi.org/10.1002/(SICI)1099-1530(199810/12)9:4%3C375::AID-PPP301%3E3.0.CO;2-0.
Isarin, R.F.B., 1997. Permafrost distribution and temperatures in Europe during the younger dryas. Permafrost Periglac 8, 313–333. https://doi.org/10.1002/(SICI)1099-1530(199709)8:3%3C313::AID-PPP255%3E3.0.CO;2-E.
Ivy-Ochs, S., Kerschner, H., Reuther, A., Maisch, M., Sailer, R., Schaefer, J., Kubik, P.V., Synal, H.-A., Schluchter, C., 2006. The timing of glacier advances in the northern European Alps based on surface exposure dating with cosmogenic ^{10}Be, ^{26}Al, ^{36}Cl, and ^{21}Ne. Geol. S. Am. S. 415, 43–60. https://doi.org/10.1130/2006.2415(04.
Ivy-Ochs, S., Kerschner, H., Maisch, M., Christl, M., Kubik, P.W., Schlüchter, C., 2009. Latest Pleistocene and Holocene glacier variations in the European Alps. Quat. Sci. Rev. 28 (21–22), 2137–2149. https://doi.org/10.1016/j.quascirev.2009.03.009.
Ivy-Ochs, S., Schaller, M., 2009. Examining processes and rates of landscape change with cosmogenic radionuclides. In: Froehlich, K. (Ed.), Radioactivity in the Environment. Elsevier, Amsterdam, pp. 231–294.
Jacko, S., Labant, S., Bátorová, K., Farkašovský, R., Ščerbáková, B., 2021. Structural

contraints of neotectonic activity in the eastern part of the Western Carpathians orogenic wedge. Quat. Int. 585, 27–43. https://doi.org/10.1016/j.quaint.2020.10.072.
Janke, J.R., Regmi, N.R., Girardino, J.R., Vitek, J.D., 2013. Rock glaciers. In: Shroder, J., Giardino, R., Harbor, J. (Eds.), Treatise on Geomorphology, Glacial and Periglacial Geomorphology, vol. 8. Academic Press, SanDiego, pp. 238–273.
Jones, D.B., Harrison, S., Anderson, K., Whalley, W.B., 2019. Rock glaciers and mountain hydrology: a review. Earth Sci. Rev. 193, 66–90. https://doi.org/10.1016/j.earscirev.2019.04.001.
Jurewicz, E., 2007. Multistage evolution of the granitoid core in Tatra Mountains. In: Kozłowski, A., Wiszniewska, J. (Eds.), Granitoids in Poland. Warsaw University, Warsaw, pp. 307–317.
Kääb, A., Gudmundsson, G.H., Hoelzle, M., 1998. Surface deformation of creeping mountain permafrost. Photogrammetric investigations on Murtèl rock glacier, Swiss Alps. In: Proceedings of the Seventh International Conference on Permafrost, pp. 531–537.
Kääb, A., Frauenfelder, R., Roer, I., 2007. On the response of rockglacier creep to surface temperature increase. Global Planet. Change 56, 172–187. https://doi.org/10.1016/j.gloplacha.2006.07.005.
Kääb, A., 2013. Rock glaciers and protalus forms. In: Elias, S.A., Mock, C.J. (Eds.), Encyclopedia of Quaternary Science, second ed. Elsevier, Amsterdam, pp. 535–541.
Kellerer-Pirklbauer, A., 2008. The Schmidt-hammer as a relative age dating tool for rock glacier surfaces: examples from Northern and Central Europe. In: Proceedings of the Ninth International Conference on Permafrost (NICOP). University of Alaska, Fairbanks, pp. 913–918.
Kellerer-Pirklbauer, A., Wangensteen, B., Farbrot, H., Etzelmüller, B., 2008b. Relative surface age-dating of rock glacier systems near Hólar in Hjaltadalur, Northern Iceland. J. Quat. Sci. 23 (2), 137–151. https://doi.org/10.1002/jqs.1117.
Kellerer-Pirklbauer, A., Lieb, G.K., Kleinferchner, H., 2012. A new rock glacier inventory of the Eastern European Alps. Aust. J. Earth Sci. 105 (2), 78–93.
Kindler, P., Guillevic, M., Baumgartner, M., Schwander, J., Landais, A., Leuenberger, M., 2014. Temperature reconstruction from 10 to 120 kyr b2k from the NGRIP ice core. Clim. Past 10, 887–902. https://doi.org/10.5194/cp-10-887-2014.
Kłapyta, P., 2009. Glacial and periglacial relief on the southern slopes of the Western Tatra Mts. (Slovakia) – the results of the first detailed geomorphological mapping of the Žiarska, Jamnicka, Račkova and Bystra Valleys. Landform Analysis 10, 50–57.
Kłapyta, P., 2011. Relative surface dating of rock glacier systems in the Žiarska Valley, the Western Tatra Mountains, Slovakia. Stud. Geomorphol. Carpatho-Balcanica 45, 89–106.
Kłapyta, P., 2013. Application of Schmidt hammer relative age dating to Late Pleistocene moraines and rock glaciers in the Western Tatra Mountains, Slovakia. Catena 111, 104–121. https://doi.org/10.1016/j.catena.2013.07.004.
Kłapyta, P., 2015. Relief of selected parts of the western Tatra mountains. In: Dabrowska, K., Guzik, M. (Eds.), Atlas of the Tatra Mountains: Abiotic Nature. TPN, Zakopane.
Kłapyta, P., Zasadni, I., Pociask-Karteczka, J., Gajda, A., Franczak, P., 2016. Late Glacial and Holocene paleoenvironmental records in the Tatra Mountains, East-Central Europe, based on lake, peat bog and colluvial sedimentary data: a summary review. Quat. Int. 415, 126–144. https://doi.org/10.1016/j.quaint.2015.10.049.
Kočický, D., 1996. Charakteristiky Snehovej Pokrývky V Oblasti Tatier V Období 1960/61-1989/90. Comenius University in Bratislava, Slovak. Unpublished diploma thesis.
Korschinek, G., Bergmaier, A., Faestermann, T., Gerstmann, U.C., Knie, K., Rugel, G., Wallner, A., 2010. A new value for the half-life of ^{10}Be by heavy-ion elastic recoil detection and liquid scintillation counting. Nucl. Instrum. Methods Phys. Res. B268 (2), 187–191. https://doi:10.1016/j.nimb.2009.09.020.
Kotarba, A., 1992. Natural environment and landform dynamics of the Tatra Mountains. Mt. Res. Dev. 105–129. https://doi.org/10.2307/3673786.
Kovács, J., Fábián, S.Á., Schweitzer, F., Varga, G., 2007. A relict sand-wedge polygon site in north-central Hungary. Permafrost Periglac 18, 379–384. https://doi.org/10.1002/ppp.600.
Krainer, K., Bressan, D., Dietre, B., Haas, J.N., Hajdas, I., Lang, K., Mair, V., Nickus, U., Reidl, D., Thies, H., Tonidandel, D., 2015. A 10,300-year-old permafrost core from the active rock glacier Lazaun, southern Ötztal Alps (South Tyrol, northern Italy). Quat. Res. (Duluth) 83 (2), 324–335. https://doi.org/10.1016/j.yqres.2014.12.005.
Králiková, S., Vojtko, R., Sliva, U., Minár, J., Fuegenschuh, B., Kovac, M., Hok, J., 2014. Cretaceous-Quaternary tectonic evolution of the Tatra Mts (Western Carpathians): constraints from structural, sedimentary, geomorphological, and fission track data. Geol. Carpathica 65 (4), 307. https://doi.org/10.2478/geoca-2014-0021.
Laustela, M., Egli, M., Frauenfelder, R., Kääb, A., Maisch, M., Haeberli, W., 2003. Weathering rind measurements and relative age dating of rockglacier surfaces in crystalline regions of the Eastern Swiss Alps. In: Proceedings of the 8th International Conference on Permafrost. Zürich, Switzerland, pp. 627–632.
Lindner, L., Dzierżek, J., Marciniak, B., Nitychoruk, J., 2003. Outline of Quaternary glaciations in the Tatra Mts.: their development, age and limits. Geol. Q. 47 (3), 269–280.
Linge, H., Nesje, A., Matthews, J.A., Fabel, D., Xu, S., 2020. Evidence for rapid paraglacial formation of rock glaciers in southern Norway from ^{10}Be surface-exposure dating. Quat. Res. (Duluth) 97, 55–70. https://doi.org/10.1017/qua.2020.10.
Makos, M., Nitychoruk, J., Zreda, M., 2013. Deglaciation chronology and paleoclimate of the pięciu stawów polskich/roztoki valley, high Tatra mountains, western Carpathians, since the last glacial maximum, inferred from ^{36}Cl exposure dating and glacier–climate modelling. Quat. Int. 293, 63–78. https://doi.org/10.1016/j.quaint.2012.01.016.
Makos, M., Rinterknecht, V., Braucher, R., Żarnowski, M., Aster Team, 2016. Glacial chronology and palaeoclimate in the Bystra catchment, western Tatra Mountains (Poland) during the late Pleistocene. Quat. Sci. Rev. 134, 74–91. https://doi.org/10.1016/j.quascirev.2016.01.004.
Makos, M., Rinterknecht, V., Braucher, R., Tołoczko-Pasek, A., Arnold, M., Aumaître, G., Bourlès, D., Keddadouche, K., 2018. Last glacial maximum and lateglacial in the polish high Tatra mountains - revised deglaciation chronology based on the ^{10}Be exposure age dating. Quat. Sci. Rev. 187, 130–156. https://doi.org/10.1016/j.quascirev.2018.03.006.
Matthews, J.A., Nesje, A., Linge, H., 2013. Relict talus-foot rock glaciers at Øyberget, upper Ottadalen, southern Norway: Schmidt hammer exposure ages and palaeoenvironmental implications. Permafrost Periglac 24, 336–346. https://doi.org/10.1002/ppp.1794.
Matthews, J.A., Winkler, S., 2022. Schmidt-hammer exposure-age dating: a review of principles and practice. Earth Sci. Rev. 230, 104038. https://doi.org/10.1016/j.earscirev.2022.104038.
Moran, A.P., Ochs, S.I., Vockenhuber, C., Kerschner, H., 2016. Rock glacier development in the northern calcareous Alps at the pleistocene-holocene boundary. Geomorphology 273, 178–188. https://doi.org/10.1016/j.geomorph.2016.08.017.
Niedźwiedź, T., 1992. Climate of the Tatra mountains. Mt. Res. Dev. 131–146. https://doi.org/10.2307/3673787.
Niedźwiedź, T., Łupikasza, E., Pińskwar, I., Kundzewicz, Z.W., Stoffel, M., Małarzewski, Ł., 2015. Variability of high rainfalls and related synoptic situations causing heavy floods at the northern foothills of the Tatra Mountains. Theor. Appl. Climatol. 119 (1), 273–284. https://doi.org/10.1007/s00704-014-1108-0.
Nemčok, A., Mahr, T., 1974. Kamenné ľadovce v tatrách (fossil rock glaciers in tatras). Geogr. časopis 26, 359–373.
Nemčok, J., Bezák, V., Biely, A., Gorek, A., Gross, P., Halouzka, R., et al., 1994. Geologická Mapa Tatier 1 : 50 000 [Geological Map of the Tatra Mts. 1 : 50 000. State Geological Institute of Dionýz Štúr, Bratislava.
Nicholas, J.W., Butler, D.R., 1996. Application of relative-age dating techniques on rock glaciers of the La Sal Mountains, Utah: an interpretation of Holocene paleoclimates. Geogr. Ann. 78, 1–18.
Obidowicz, A., 1996. A Late glacial-Holocene history of the formation of vegetation belts in the Tatra Mts. Acta Paleobot 36 (2), 159–206.
Orvošová, M., Deininger, M., Milovský, R., 2014. Permafrost occurrence during the last permafrost maximum in the western carpathian mountains of Slovakia as inferred from cryogenic cave carbonate. Boreas 43, 750–758. https://doi.org/10.1111/bor.12042.
Palacios, D., Andrés, N., López-Moreno, J., García-Ruiz, J.M., 2015. Late Pleistocene deglaciation in the upper gállego valley, central pyrenees. Quat. Res. (Duluth) 83, 397–414. https://doi.org/10.1016/j.yqres.2015.01.010.
Palacios, D., Gómez-Ortiz, A., Andrés, N., Salvador, F., Oliva, M., 2016. Timing and new geomorphologic evidence of the last deglaciation stages in Sierra Nevada (southern Spain). Quat. Sci. Rev. 150, 110–129. https://doi.org/10.1016/j.quascirev.2016.08.0127.
Palacios, D., Rodríguez-Mena, M., Fernández-Fernández, J.M., Schimmelpfennig, I., Tanarro, L.M., Zamorano, J.J., Andrés, N., Úbeda, J., Sæmundsson, Þ., Brynjólfsson, S., Oliva, M., ASTER Team., 2021. Reversible glacial-periglacial transition in response to climate changes and paraglacial dynamics: a case study from Héðinsdalsjökull (northern Iceland). Geomorphology 388, 107787. https://doi.org/10.1016/j.geomorph.2021.107787.
Pánek, T., Engel, Z., Mentlík, P., Braucher, R., Břežný, M., Škarpich, V., Zondervan, A., 2016. Cosmogenic age constraints on post-LGM catastrophic rock slope failures in the Tatra Mountains (Western Carpathians). Catena 138, 52–67. https://doi.org/10.1016/j.catena.2015.11.005.
Pánek, T., Minár, J., Vitovič, L., Břežný, M., 2020. Post-LGM faulting in central Europe: LiDAR detection of the >50 km-long sub-Tatra fault, western Carpathians. Geomorphology 364, 107248. https://doi.org/10.1016/j.geomorph.2020.107248.
Rasmussen, S.O., Bigler, M., Blockley, S.P., Blunier, T., Buchardt, S.L., Clausen, H.B., Cvijanovic, I., Dahl-Jensen, D., Johnsen, S.J., Fischer, H., Gkinis, V., Guillevic, M., Hoek, W.Z., Lowe, J.J., Pedro, J.B., Popp, T., Seierstad, I.K., Steffensen, J.P., Svensson, A.M., Vallelonga, P., Vinther, B.M., Walker, M.J.C., Wheatley, J.J., Winstrup, M., 2014. A stratigraphic framework for abrupt climatic changes during the Last Glacial period based on three synchronized Greenland ice-core records: refining and extending the INTIMATE event stratigraphy. Quat. Sci. Rev. 106, 14–28. https://doi.org/10.1016/j.quascirev.2014.09.007.
Refsnider, K.A., Brugger, K.A., 2007. Rock glaciers in central Colorado, U.S.A., as indicators of late- Holocene climate change: a lichenometric study using Rhizocarpon subgenus Rhizocarpon. Arctic Antarct. Alpine Res. 39, 127–136. https://doi.org/10.1657/1523-0430(2007)39[127:RGICCU]2.0.CO;2.
RGIK, 2022. Towards Standard Guidelines for Inventorying Rock Glaciers: Practical Concepts (Version 2.0). IPA Action Group Rock glacier inventories and kinematics, p. 10.
Rode, M., Kellerer-Pirklbauer, A., 2012. Schmidt-hammer exposure-age dating (SHD) of rock glaciers in the Schöderkogel-Eisenhut area, Schladminger Tauern Range, Austria. Holocene 22 (7), 761–771. https://doi.org/10.1177/0959683611430410.
Rodríguez-Rodríguez, L., Jiménez-Sánchez, M., Domínguez-Cuesta, M.J.,

Rinterknecht, V., Pallas, R., Bourles, D., 2016. Chronology of glaciations in the Cantabrian Mountains (NW Iberia) during the Last Glacial Cycle based on in situ-produced ^{10}Be. Quat. Sci. Rev. 138, 31–48. https://doi.org/10.1016/j.quascirev.2016.02.027.

Rodríguez-Rodríguez, L., Jiménez-Sánchez, M., Domínguez-Cuesta, M.J., Rinterknecht, V., Pallàs, R., AsterTeam, 2017. Timing of last deglaciation in the Cantabrian Mountains (Iberian Peninsula; North Atlantic Region) based on in situ-produced ^{10}Be exposure dating. Quat. Sci. Rev. 171, 166–181. https://doi.org/10.1016/j.quascirev.2017.07.012.

Rybníčková, E., Rybníček, K., 2006. Pollen and macroscopic analyses of sediments from two lakes in the High Tatra mountains, Slovak. Veg. Hist. Archaeobotany 15, 345–356.

Santos-González, J., González-Gutiérrez, R.B., Redondo-Vega, J.M., Gómez-Villar, A., Jomelli, V., Fernández-Fernández, J.M., Andrés, N., García-Ruiz, J.M., Peña-Pérez, S.A., Melón-Nava, A., Oliva, M., Álvarez-Martínez, J., Charton, J., , ASTER Team, Palacios, D., 2022. The origin and collapse of rock glaciers during the Bølling-Allerød interstadial: A new study case from the Cantabrian Mountains (Spain). Geomorphology 401, 108112. https://doi.org/10.1016/j.geomorph.2022.108112.

Scapozza, C., Lambiel, C., Reynard, E., Fallot, J.M., Antognini, M., Schoeneich, P., 2010. Radiocarbon dating of fossil wood remains buried by the Piancabella rock glacier, Blenio Valley (Ticino, Southern Swiss Alps): implications for rock glacier, treeline and climate history. Permafrost Periglac 21, 90–96. https://doi.org/10.1002/ppp.673.

State Geological Institute of Dionýz Štúr, 2013. Geological map of Slovakia M 1:50 000. http://apl.geology.sk/gm50js/. (Accessed 6 March 2021).

Steinemann, O., Reitner, J.M., Ivy-Ochs, S., Christl, M., Synal, H.A., 2020. Tracking rockglacier evolution in the Eastern Alps from the Lateglacial to the early Holocene. Quat. Sci. Rev. 241, 106424. https://doi.org/10.1016/j.quascirev.2020.106424.

Stone, J.O., 2000. Air pressure and cosmogenic isotope production. J. Geophys. Res. 105 (B10), 23753–23759. https://doi.org/10.1029/2000JB900181.

ÚGKK, S.R., 2018. Airborne Laser Scanning and DEM 5.0. Site No. 26 (Tatra Mts.). The Geodesy, Cartography and Cadastre Authority of the Slovak Republic (Bratislava).

Ustrnul, Z., Walawender, E., Czekierda, D., Šťastný, P., Lapin, M., Mikulová, K., 2015. Precipitation and snow cover. In: Dabrowska, K., Guzik, M. (Eds.), Atlas of the Tatra Mountains: Abiotic Nature. TPN, Zakopane.

Uxa, T., Mida, P., 2017. Rock glaciers in the western and high Tatra mountains, western Carpathians. J. Maps 13 (2), 844–857. https://doi.org/10.1080/17445647.2017.1378136.

Vermeesch, P., 2012. On the visualisation of detrital age distributions. Chem. Geol. 312–313, 190–194. https://doi.org/10.1016/j.chemgeo.2012.04.021.

Vasile, M., Vespremeanu-Stroe, A., Pascal, D., Braucher, R., Pleșoianu, A., Popescu, R., Etzelmüller, B., ASTER Team., 2022. Rock walls distribution and Holocene evolution in a mid-latitude mountain range (the Romanian Carpathians). Geomorphology 413, 108351. https://doi.org/10.1016/j.geomorph.2022.108351.

Vespremeanu-Stroe, A., Urdea, P., Popescu, R., Vasile, M., 2012. Rock glacier activity in the Retezat mountains, Southern Carpathians, Romania. Permafost. Periglac. 23, 127–137. https://doi.org/10.1002/ppp.1736.

Vitovič, L., Minár, J., Pánek, T., 2021. Morphotectonic configuration of the Podtatranská Kotlina Basin and its relationship to the origin of the Western Carpathians. Geomorphology 394, 107963. https://doi.org/10.1016/j.geomorph.2021.107963.

Ward, G.K., Wilson, S.R., 1978. Procedures for comparing and combining radiocarbon age determinations: a critique. Archaeometry 20 (1), 19–31.

Whalley, W.B., Martin, H.E., 1992. Rock glaciers: II models and mechanisms. Prog. Phys. Geogr. 16 (2), 127–186.

Žák, K., Richter, D.K., Filippi, M., Živor, R., Deininger, M., Mangini, A., Scholz, D., 2012. Coarsely crystalline cryogenic cave carbonate – a new archive to estimate the Last Glacial minimum permafrost depth in Central Europe. Clim. Past. 8, 1821–1837. https://doi.org/10.5194/cp-8-1821-2012.

Zasadni, J., Kłapyta, P., 2009. An attempt to assess the modern and the Little Ice Age climatic snowline altitude in the Tatra Mountains. Landform Analysis 10, 124–133.

Zasadni, J., Kłapyta, P., 2016. From valley to marginal glaciation in alpine-type relief: Lateglacial glacier advances in the Pięć Stawów Polskich/Roztoka Valley, High Tatra Mountains, Poland. Geomorphology 253, 406–424. https://10.1016/j.geomorph.2015.10.032.

Zasadni, J., Kłapyta, P., Broś, E., Ivy-Ochs, S., Świąder, A., Christl, M., Balážovičová, L., 2020. Latest Pleistocene glacier advances and post-Younger Dryas rock glacier stabilization in the Mt. Kriváň group, High Tatra Mountains, Slovakia. Geomorphology 358, 107093. https://doi.org/10.1016/j.geomorph.2020.107093.

Zasadni, J., Kłapyta, P., Makos, M., 2022. The evolution of glacial landforms in the Tatra Mountains during the Bølling-Allerød Interstadial. In: Palacios, D., Hughes, P.D., Garcia-Ruiz, J.M., de Andrés, N. (Eds.), European Glacial Landscapes: the Last Deglaciation. Elsevier. https://doi.org/10.1016/C2020-0-00404-4.

Żmudzka, E., Nejedlík, P., Mikulová, K., 2015. Temperature, thermal indices. In: Dabrowska, K., Guzik, M. (Eds.), Atlas of the Tatra Mountains: Abiotic Nature. TPN, Zakopane.